Contents lists available at Egyptian Knowledge Bank

Labyrinth: Fayoum Journal of Science and Interdisciplinary Studies

Journal homepage: https://lfjsis.journals.ekb.eg/

The therapeutic potential of utilizing mesenchymal stem cell transplantation for remedying premature ovarian failure in female rats.

Nehal Sobhy [a], Ahmed Atwa [b,*], Abdel Kareem M Abdel Latif [a], Sayed Bakry [b]

[a] Zoology Department, Faculty of Science, Fayoum University, El Fayoum 63514, Egypt.
[b] Center for Genetic Engineering- Al-Azhar University, Nasr City, Cairo 11884, Egypt.

ARTICLE INFO

Keywords:
Cyclophosphamide
Mesenchymal Stem Cells
Chemotherapy
Premature Ovarian Failure

ABSTRACT

Chemotherapy severely reduces primordial follicles in cancer survivors, leading to premature ovarian failure (POF). This study investigates the potency of bone marrow-derived mesenchymal stem cells (BM-MSCs) on POF induced by cyclophosphamide chemotherapy. Twenty-one female albino Sprague Dawley rats were divided into three equal groups (n=7): Group 1 served as the negative control, group 2 was the positive control receiving intraperitoneal (IP) injections of cyclophosphamide (CPA) (50 mg/kg) once, followed by CPA (8 mg/kg) daily for 14 days, and group 3 received intravenous (IV) BM-MSC therapy ($1x10^6$ cells) after POF induction by CPA and were sacrificed after 4 weeks. Hormonal FSH, LH, E2, and progesterone levels were assessed using ELISA, and primordial follicles were quantified to evaluate follicle reserve. Ovarian structure was assessed histomorphologically, and morphometric measurements and statistical analysis were conducted. The homing of BM-MSCs in the ovary was verified by analyzing PKH-26 labelled BM-MSCs under a fluorescent microscope. Hormonal analysis showed increased FSH levels and decreased E_2 and progesterone levels following CPA administration, with near-normal restoration of hormonal levels after BM-MSC therapy. CPA caused significant loss of primordial follicles, stromal blood vessel damage, and notable fibrosis. In contrast, BM-MSC therapy facilitated ovarian folliculogenesis and mitigated these histological changes. Specifically, hormone measurements indicated decreased E2 and progesterone levels and increased FSH levels post-CPA treatment. After BM-MSC therapy, hormonal levels approached normal. Cyclophosphamide caused significant primordial follicle loss, stromal blood vessel damage, and substantial fibrosis, whereas BM-MSC therapy restored ovarian folliculogenesis and reduced these histological alterations. Our results suggest that BM-MSCs possess notable regenerative effects on the maturation of follicles in cyclophosphamide-induced ovarian failure. In conclusion, BM-MSCs demonstrate reparative effects on follicle maturation in ovarian damage caused by Cyclophosphamide, suggesting their potential therapeutic role in mitigating chemotherapy-induced POF.

1. Introduction

A couple with infertility is unable to achieve pregnancy within a year or six months despite engaging in regular, unprotected sexual contact three to four times per week [1]. This condition may result from medical issues that interfere with ovulation, damage the fallopian tubes, or cause hormonal imbalances.

Premature ovarian failure (POF) is a type of ovarian dysfunction marked by menstrual irregularities, ovarian atrophy, diminished sexual function, and reduced fertility in women between 40 years of age and puberty. POF significantly affects endocrine balance and female reproductive health, making it a leading cause of female infertility [2].

Stem cells throughout human development and lifespan are undifferentiated cells capable of self-renewal, producing identical cells through division and differentiating into various cell types [3]. Research has investigated the potential of stem cells in fertility preservation [4,5]. Moreover, the human placenta and its derivatives have shown capabilities in immune system regulation, hepatocyte protection and regeneration, hormonal balance maintenance in women, and alteration of brain monoamine oxidase activity [6].

Animal models of premature ovarian insufficiency (POI), such as those utilizing POF mice and rats, serve as valuable tools for elucidating this condition's underlying genetic and molecular mechanisms and informing the development of innovative therapeutic approaches. POI models can be

*Corresponding author.
E-mail address: ahmed.atwa@azhar.edu.eg (A. Atwa); Tel.: +20842029465

DOI: 10.21608/IFJSIS.2024.297925.1081
Received 17 June 2024; Received in revised form 15 July 2024; Accepted 20 July 2024
Available online 21 July 2024

induced chemically using agents like Cyclophosphamide and Cisplatin via intraperitoneal (i.p.) administration or busulfan and murine ZP3 330–342 peptides (ZP3) by tail-vein (intravenous, i.v) injection; vaginal smears are usually used for confirmation [7].

Cyclophosphamide (CPA) is commonly used to treat various cancers, including melanomas, breast and pediatric cancers. Still, it carries a significant risk of inducing ovarian failure [8]. Among chemotherapy drugs, CPA is notably associated with the highest risk of infertility due to its severe impact on ovarian follicles, leading to premature ovarian insufficiency (POI) [9].

Promising evidence suggests that patients who undergo bone marrow (BM) transplants may unexpectedly regain ovarian function and fertility [10]. This restoration is thought to be linked to the regenerative properties of mesenchymal stem cells (MSCs). Unfortunately, the notion that ovarian or mesenchymal stem cells can facilitate neo-oogenesis remains contentious, with ongoing scientific debate and conflicting findings [11].

The present study aims to investigate the therapeutic potential of mesenchymal stem cell (MSC) transplantation in female rats with experimentally induced premature ovarian failure (POF). This proof-of-concept study is designed to evaluate the efficacy of BM-MSCs in treating CPA-produced ovarian insufficiency in a rat model.

2. Materials and Methods:

2.1. Ethical Approval, POF model establishment and Experimental Design

Cyclophosphamide (CPA), commercially known as Endoxan®, was procured in 1g vials from Baxter Oncology GmbH, Halle, Germany. For administration, CPA was reconstituted in phosphate-buffered saline (PBS). The rats received an initial intraperitoneal (I.P.) injection of CPA at a dosage of 50 mg/kg. This was followed by daily I.P. injections of 8 mg/kg for 14 consecutive days, depending on the methodology outlined by Aboutalebi et al., [12]. Following the rules for the Care and Use of Laboratory Animals, the animal studies were carried out at Al-Azhar University's Animal House. Under permission number AEC 2320, all operations were authorized by Fayoum University's Institutional Animal Care and Use Committee (FU-IACUC). Twenty-one adult female Sprague Dawley (SD) rats weighing approximately 200±20 grams were acquired from the VACSERA animal facility in Cairo, Egypt. The rats were provided ad libitum entry to water, food, and subsequently randomized into various experimental groups, as outlined in Table 1.

Table 1. The experimental design for different studied groups and the duration of each group of 21 female rats. They randomly divided into 3 groups after vaginal smear for the Estrous cycle (n=7):

Group	Description
Group 1, (GI)	Female rats were administered a standard diet and subsequently euthanized via an intraperitoneal injection of 80 mg/kg sodium pentobarbital upon conclusion of the experiment.
Group CPA, (GII)	They were then subjected to a 50 mg/kg dose of (CPA), followed by daily intraperitoneal injections of CPA at 8 mg/kg for a period of 14 days.
Group MSCs, (GIII)	Each rat received a single intravenous transplantation of 1×10^6 (MSCs). After 4 weeks, they were euthanized via intraperitoneal injection of 80 mg/kg sodium pentobarbital.

2.2. Hormonal Profiling

The ELISA technique (Dynatech Microplate Reader Model MR 5000) was used to measure the concentrations of serum follicle-stimulating hormone (FSH), progesterone, luteinizing hormone (LH), and estradiol (E2). Reagent kits were obtained from from Biosource, USA [13].

2.3. Isolation of Mesenchymal Stem Cells from Rat Bone Marrow (BM-MSCs)

An intraperitoneal injection of sodium pentobarbital (30 mg/kg) was used to euthanize six-week-old female white albino rats. Before bone marrow extraction, the tibiae and femurs were flushed with Dulbecco's Modified Eagle's Medium (DMEM), containing 10% fetal bovine serum (Gibco BRL, Karlsruhe, Germany). Using a Ficoll-Paque density gradient (Pharmacia), nucleated cells were isolated and resuspended in a 1% penicillin-streptomycin-containing medium (Gibco BRL). Large colonies reached 80-90% confluence after 12-14 days of incubation at 37°C in a humidified atmosphere with 5% CO_2. A 5-minute dissociation procedure with 0.25% trypsin in 1 mM EDTA (Gibco BRL) was performed after incubation with PBS. A serum-supplemented medium was used to resuspend the cells and transfer them to a falcon culture flask of 50 cm^2 for first-passage culture [14]. Mesenchymal stem cells (MSCs) were characterized by their adherence properties and spindle-shaped morphology. Cells were subjected to three passages to obtain enough MSCs for transplantation. After trypsinization, cells were collected into a 15 ml Falcon tube and centrifuged at 480 g for 5 minutes. Cell viability was evaluated using the trypan blue exclusion assay [15].

2.4. PKH26-labelled BM- MSCs

When cells reached 80–90% confluence, adherent hAMSCs were trypsinized and centrifuged to obtain cellular pellets and then resuspended in 1 ml PBS. First, 2.0×10^6 cells were incubated with 250 µl 4.0 × 10−6 mol/L PKH26 at room temperature for 5 min. The reaction was stopped with 250 µl FBS and diluted with an equal amount of 10% FBS. The cells were centrifuged and resuspended in 10 mL complete medium and then washed twice with PBS. The morphology of PKH26-labelled hAMSCs was observed under an inverted phase-contrast fluorescence microscope, and the percentage of PKH26 marker cells was detected by flow cytometry.

2.5. Histological and Immunofluorescence examination

After euthanasia, the ovaries were immediately excised and fixed in 10% formalin saline for 24 to 48 hrs. A graded ethanol series dehydrated the tissues, which were then cleared in xylene and embedded in paraffin. Histopathological analysis was performed using sections cut with a Leica rotary microtome (Germany) stained with hematoxylin and eosin.

2.6. Tracking of PKH26-Labeled BM-MSCs

To identify the location and fate of transplanted MSCs in ovarian tissues, immunofluorescence analysis was conducted. Three rats from each group were randomly selected and euthanized at 7 and 14 days post-transplantation of PKH-26-labeled MSCs. One ovary from each rat was harvested and immersed in a 20% sucrose solution for 2 hours. The ovaries were then embedded in a cryoembedding medium and sectioned into 5 μm slices using a cryostat. Fluorescence microscopy (Leica Biosystems, Germany) was employed to visualize the sections. The presence and distribution of PKH-26-labeled MSCs were identified by detecting red fluorescence signals within the ovarian tissue.

2.7. Morphometric Analysis

The quantitative analysis of the average number of primordial follicles per group (± SD) was conducted using Image-J software.

2.8. Statistical Analysis

Version 20 of the SPSS program was used for the statistical analysis. The data was analyzed using a one-way analysis of variance, and the findings were presented as mean values and standard errors (± S.E.). P values less than 0.05 were considered statistically significant.

3. Results

3.1. MSCs recovered the oestrus cycle

The estrous cycle was assessed following CPA administration to validate the POF model's efficacy. Vaginal smears were examined without staining using an inverted phase contrast microscope (Olympus, Tokyo, Japan). During the estrous phase, cornified cells indicated estrogenic activity and the absence of progression to the subsequent metaestrous, diestrous, and proestrous phases. This observation marked the initiation of treatment, as detailed in Table 2. Subsequently, the oestrous cycle was monitored daily throughout the experiment post-administration of BM-MSCs to evaluate the treatment efficacy. The results were analyzed as follows: The table's cells contain mean values alongside their respective standard deviations (±) for each parameter and group. Statistically significant differences between groups for each parameter are denoted by letters (a, b, c), with distinct lower-case letters indicating significant differences. The table delineates estrogenic activity across distinct groups during the estrous cycle, encompassing the Control, CPA, and BM-MSCs (groups. Regarding the estrous cycle parameter, the Control group demonstrated significantly elevated values compared to the CPA and BM-MSC groups. This pattern of significant differences persisted consistently across all evaluated parameters and groups, offering crucial insights into the variations in estrogenic activity throughout the oestrous cycle under diverse experimental conditions.

Table 2. shows the indications of estrogenic activity during the estrous cycle.

Parameters / Groups	Proestrous	Estrous	Metaestrous	Diestrous
Control (GI)	49.2 ± 1.1a	30.8 ± 1.3a	5.6 ± 0.6a	6.9 ± 0.3a
CPA (GII)	15.8 ± 0.5b	11.4 ± 0.4b	17.1 ± 1.2b	14.2 ± 0.5b
BM-MSCs (GIII)	29.7 ± 1.3c	17.4 ± 1.03c	9.1 ± 0.3c	7.8 ± 0.7a

3.2. Body weight changes

Table 3 presents the variations in body weight across different experimental groups, specifically the GI, GII (an intervention or treatment), and GIII (another treatment group). Body weights for each group are indicated as mean ± SE. The letters (a, b, c) indicate significant differences between groups, emphasizing which groups show statistically significant differences in body weight changes. The statistical analysis suggests that the GII group experienced a more substantial body weight reduction than the GI and GIII groups.

Table 3. Body weight changes

Parameter	Control (GI)	CPA (GII)	BM-MSCs (GIII)
Body weight	199.8 ± 4.1a	139.8 ± 3.9b	159.1 ± 3.7c

The Table's cells contain mean values alongside their respective standard error for each parameter and group. Statistically significant differences between groups for each parameter are denoted by letters (a, b, c), with distinct lower-case letters indicating significant differences.

3.3. Hormonal profile

The study employed ELISA kits to quantify E2, Progesterone, LH, and FSH serum levels. The findings reveal substantial variations in these hormonal levels among the different experimental groups, as detailed in Table 4. Firstly, FSH levels were markedly elevated in the GII-treated group relative to the control group, whereas the GIII-applied group demonstrated significantly lower FSH levels than GII. This indicates that GII had the highest FSH levels observed six weeks post-chemotherapy. Secondly, LH levels significantly rose in the GII compared to the control group but were reduced in the GIII. As a result, six weeks following chemotherapy, GII exhibited the highest LH levels. Thirdly, estradiol levels significantly declined in the GII relative to the GI; however, they significantly rose higher in the GIII. Consequently, GII displayed the lowest Estradiol levels after six weeks of chemotherapy. Finally, progesterone levels were significantly reduced in the GII than the GI, but they rose significantly in the GIII. Therefore, six weeks after chemotherapeutic intervention, GII showed the lowest progesterone levels. These results collectively suggest that chemotherapeutic treatment elevates FSH and LH levels while reducing estradiol and Progesterone levels and that treatment with GIII can mitigate these effects to varying degrees.

Table 4. Hormonal profile

Parameter	Control (GI)	CPA (GII)	BM-MSCs (GIII)
Progesterone	5.6 ± 0.23a	1.7 ± 0.13b	2.3 ± 0.16c
Estradiol	57.9 ± 2.3a	16.4 ± 1.1b	35.2 ± 0.48c
luteinizing hormone	0.23 ± .007a	0.8 ± .04b	0.61 ± .03d
Follicle stimulating hormone	0.34 ± .02a	0.91 ± .04b	0.56 ± .05c

The table's cells contain mean values alongside their respective standard error for each parameter and group. Statistically significant differences between groups for each parameter are denoted by letters (a, b, c), with distinct lower-case letters indicating significant differences.

3.4. Morphometric analysis of primordial follicles

3.4.1. Primordial diameter and count

Our morphometric analysis evaluated the primordial diameter and count across three experimental groups: Control, CPA, and BM-MSCs. The Ccontrol group exhibited a primordial diameter averaging 121.2 ± 4.6 units. In contrast, the CPA group demonstrated a significantly reduced average diameter of 68.3 ± 3.3 units, whereas the BM-MSCs group showed an average diameter of 106.4 ± 1.2 units. Regarding the primordial count, the control group averaged 7.2 ± 0.4, while the CPA group had a markedly lower average of 3.5 ± 0.26. The BM-MSCs group presented an intermediate value, with an average count of 5.4 ± 0.17.

3.4.2. Comparative analysis

The comparative data underscore significant variations in both primordial diameter and count among the experimental groups. The exposure to CPA and the administration of MSCs significantly influenced the size and number of primordial follicles than the control group, as summarized in Table 5. Table 5 delineates the mean values and standard deviations for both primordial diameter (Pd) and primordial count (Pc) across the different experimental conditions. Groups sharing the same letter exhibit no significant difference in their measurements, whereas different letters denote significant differences. This detailed morphometric analysis highlights the impact of CPA and BM-MSCs on primordial follicle morphology, providing insights into their potential therapeutic implications.

Table 5. Presents the mean values of primordial diameter and counts

Parameter	Control (GI)	CPA (GII)	BM-MSCs (GIII)
Primordial diameter (PD)	128.2 ± 4.6a	71.3 ± 3.4b	104.4 ± 1.3c
Primordial count (PC)	7.0 ± 0.3a	3.3 ± 0.28b	5.3 ± 0.18c

The Table's cells contain mean values alongside their respective standard error for each parameter and group. Statistically significant differences between groups for each parameter are denoted by letters (a, b, c), with distinct lower-case letters indicating significant differences.

3.5. Histological and histopathological observations

Histopathological examination was conducted in all groups to evaluate the effect of BM-MSC transplantation. In the control group, the ovaries displayed numerous healthy follicles at various stages, including primordial, primary, secondary, and antral follicles (Fig. 1a-f). Microscopic examination of the ovaries in Group I revealed a normal histological structure. Primal follicles with central oocytes and nuclei were present, along with follicles at various developmental stages (Fig. 1A). Primary follicles exhibited larger oocytes (Fig. 1B), and secondary follicles (Fig. 1C) featured large oocytes encircled by a cuboidal cell layer, zona pellucida (ZP), multiple layers of granulosa cells (GCs), and an antral cavity (Fig. 1D). Each follicle was surrounded by flat stromal cells. Additionally, several mature Graafian follicles (GF) with intact walls were observed (Fig. 1E). The cumulus oophorus (CO) was prominently observed, containing a well-defined oocyte with a distinct nucleus, enveloped by GCs, Corona radiata (CR), and ZP. The corpus luteum (CL), depicted in Fig. 1F, contained large acidophilic cells with a faint stain. Ovarian sections showed a cortex with multiple corpora lutea, a Graafian follicle, smaller primordial follicles, and secondary follicles within the cortical region.Conversely, the ovaries of CPA-induced POF model rats showed signs of atrophy, characterized predominantly by interstitial cells in a fibrous matrix and a reduced number of follicles at each developmental stage. The POF model rats had fewer well-developed follicles and numerous atretic follicles compared to the control group. Although follicle development at all stages was partially restored in POF rats, they did not reach normal levels within 28 days post-BM-MSCs transplantation. Notably, follicles at all developmental stages with abundant granulosa cells (Fig. 2, histopathological details are provided for each graph) showed a significant increase compared to the POF model group. After 28 days, the ovarian morphology of BM-MSCs transplanted rats closely resembled that of normal ovaries in the control group. Many mature oocytes were surrounded by several layers of squamous granulosa cells, with the oocyte-corona-cumulus complex and pellucid zone all observed

in mature oocytes.

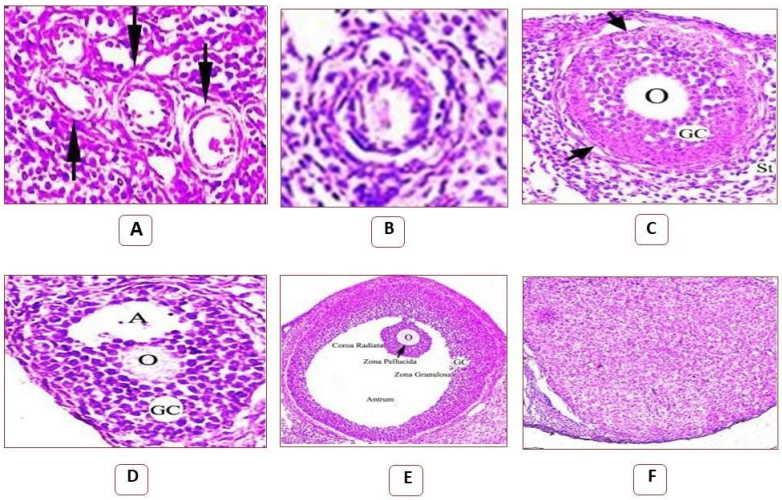

Fig. 1. Photomicrographs showing different follicle stages in normal ovarian structure histology stained with hematoxylin and eosin (magnification ×40).

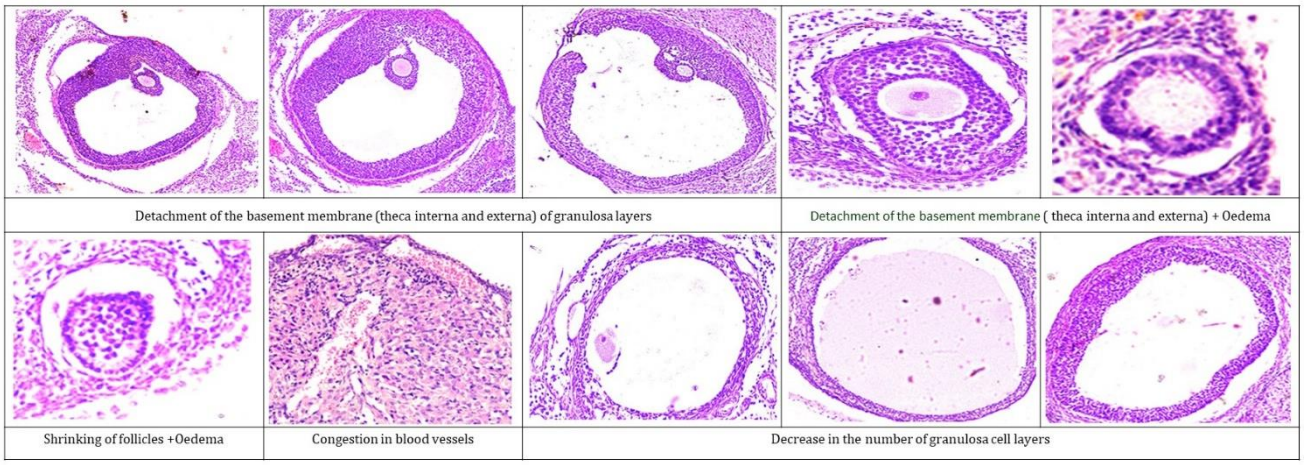

Fig. 2. The ovarian pathological alterations were assessed using H&E staining in the CPA group 28 days following POF induction (magnification ×40)

Table 6. Histopathological and follicular changes in POF rats showing impact of MSCs therapy.

Histopathological lesions								
	Distortion & degenerated primordial follicles and uni-laminar primary follicles			Shrinkage	Biantral follicle	Separation	Cyst	Degenerated corpos luteum
Control (GI)	-	-	-	-	-	-	-	-
CPA(GII)	+++	+++	+++	+++	+++	+++	++++	+++
BM-MSCs	++	++	++	++	++	++	++	++

The data in Table 6 illustrates significant histopathological changes in the ovaries of female rats in the POI group (Group II). This group exhibited a marked reduction in the total follicle count, especially in antral and mature follicles (0.4 ± 0.41 and 0.2 ± 0.22, respectively), as well as primordial and primary follicles (0.5 ± 0.52), compared to both the GI and the GIII. Observations of Graafian follicles in the POI group showed signs of oedema, cellular disintegration, compromised layer integrity, and absence of the CO. GCs in this group displayed shrinkage and pyknotic nuclei. Additionally, there was a significant rise in atretic follicles in the POI group (2.8 ± 0.63) compared to the other groups. The ovarian medulla in the POI group exhibited extensive damage with significant oedema. However, many of these histopathological abnormalities were notably ameliorated in the GIII.

3.6. Identification of BM-MSCs labelled utilizing the PKH26 fluorescent dye

In this investigation, female rats were done BMMSCs labelled with PKH-26 fluorescent dye. Then, we examined their localization within ovarian tissue using a fluorescent microscope. The utilization of PKH-26 labelling facilitated the straightforward monitoring of the administered stem cells. The conspicuous red autofluorescence is evident in unstained ovarian sections (see Fig. 3, a-b), corroborating the labelled BM-MSCs within the tissue and confirming successful implantation. This approach substantiated homing, underscoring the integration of the administered stem cells into the ovarian tissue. The detection of red fluorescence within the tissue substantiated the presence of the labelled stem cells, thereby validating their engraftment.

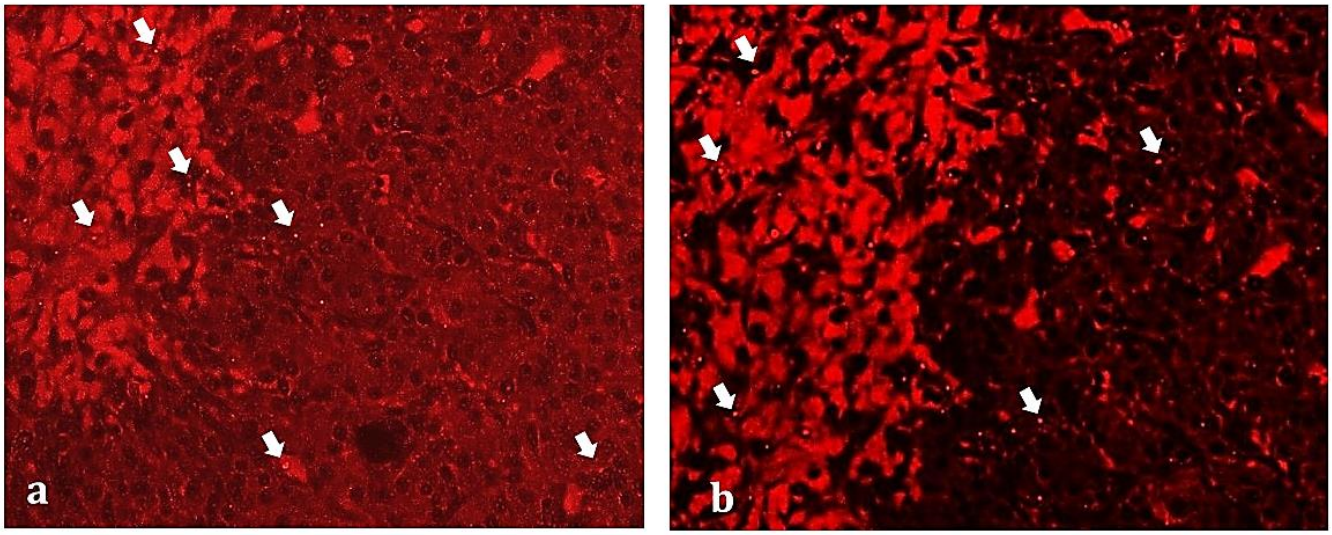

Fig. 3. Tracking of MSCs in vivo in MSCc rats (group III) . (a, b) MSCs labeled with PKH26 exhibited red fluorescence.

Post-transplantation, these MSCs were detectable in the MSC rats ovaries under both bright and dark fields using a fluorescence microscope at 100x magnification.

4. Discussion

This investigation utilized vaginal smears and hormonal assays to validate the diagnosis of ovarian failure (OF). Results revealed elevated levels of FSH and LH, along with decreased concentrations of E2 and progesterone in chemotherapy-treated subjects compared to controls, indicating of presence. A reliable method for assessing ovarian reproductive lifespan, fertility estimation, and premature ovarian failure (POF) risk involves analyzing E2, FSH, and LH levels in serum [16].

POF exhibits a distinct endocrine profile believed to influence ovarian follicle apoptotic pathways, leading to abnormal follicular atresia. Granulosa cells (GCs) predominantly secrete estrogen and progesterone, vital for proliferation and apoptosis prevention via autocrine mechanisms. Chemotherapeutic agents inhibit GC synthesis, reducing estrogen production and disrupting the pituitary-hypothalamus negative feedback loop, increasing FSH secretion [17]. Ovarian specimens from chemotherapy-treated subjects displayed shrunken ovaries with significant follicle loss and increased atretic follicles one week later. Although some follicles were visible after five weeks of chemotherapy, many had degenerated, indicating halted folliculogenesis post-chemotherapy. This phenomenon, observed previously, suggests that chemotherapy eliminates oocytes and disrupts the impeding follicular renewal, germ cell niche, and follicular renewal [18]. Consistent with previous findings, our study demonstrated in vivo transplanted BM-MSCs migration and localization within the ovarian stroma, granulosa cell layer, and theca cell layer. Despite the limited number of transplanted cells, beneficial effects were observed, as MSCs exert direct and paracrine/autocrine effects, contributing to tissue recovery [4,19–21]. Research indicates a decrease in primordial follicles 48 hours post-Cyclophosphamide® administration. Our findings suggest that in vivo transplanted BM-MSCs partially mitigate this reduction, particularly evident in group 3, while Cyclophosphamide® inhibits cell division, BM-MSCs promote proliferation [22–24]. The mechanism underlying follicle disappearance post-chemotherapy remains unclear but may involve direct cytotoxic effects on apoptotic and oocytes demise of primordial follicles, hindering folliculogenesis and accelerating ovarian ageing [25].

The primary challenge of MSC-based therapy lies in stem cell delivery to the injury site, termed "homing," which is essential for therapeutic efficacy. MSCs produce paracrine factors enhancing regeneration, requiring successful delivery to the target organ. Previous research suggests MSC migration to various organs following intravenous transplantation, with mechanisms inducing migration and homing still debated [26]. Factors influencing MSC homing include organ damage severity and vascular abundance, facilitating cell homing akin to immune cells via surface adhesion molecules. Various factors, such as FGF, HGF and TNF-α, may regulate MSC homing [27].

Studies investigating MSC homing in premature ovarian insufficiency (POI) suggest MSCs mainly migrate to the medulla and ovarian hilum post-intravenous administration, with limited migration to the cortex and no migration to the follicle. This implies settlement in the ovary's interstitium, potentially restoring follicular function through their secretory function, supported by ovarian hilum and medulla vascularization [28]. Additionally, adipose-derived MSCs (ADSCs) engraft or migrate to the thecal layers while the follicles foster follicular growth [19]. Fluorescent microscope observations confirmed BM-MSCs' homing in treated female rats' ovarian tissues. Histological findings support that MSCs contribute to the restoration of ovarian function without differentiating into granulosa cells or oocytes, acting as crucial microenvironmental components [4,19,20,29]. MSCs' capacity for differentiation and secretion enables them to reach target areas and exert therapeutic and regulatory effects [26]. In our examination, female rats administered varying doses of CPA orally exhibited toxicity signs and clinical presentations, including diarrhea, palpitations, reduced food and water intake, and alopecia. Moreover, a significant reduction in body weight was observed in female rats within the CPA group compared to the GI and GIII-treated groups. Conversely, the GIII-treated group displayed a notable rise in body weight. Comparable adverse effects, such as alopecia, cytopenia, hemorrhagic cystitis, amenorrhea, and mild to moderate nausea and vomiting, have been documented in various studies and clinical trials involving Cyclophosphamide® administration [30]. In our examination, female rats administered varying doses of CPA orally exhibited toxicity signs and clinical presentations, including diarrhea, palpitations, reduced food and water intake, and alopecia. Moreover, a significant reduction in body weight was observed in female rats within the GII group compared to the GI and GIII-treated groups. Conversely, the GIII-treated group displayed a notable increase in body weight. Comparable adverse effects, such as alopecia, cytopenia, hemorrhagic cystitis, amenorrhea, and mild to moderate nausea and vomiting, have been documented in various studies and clinical trials involving Cyclophosphamide® administration [31].

Hormonal assessment plays a pivotal role in evaluating ovarian health, fertility status, and the risk of POF. Diminished ovarian reserve and reduced levels of ovarian sex hormones typify primary ovarian insufficiency (POI), contributing to premature menopause and accelerated ovarian function decline. Blood assays for E2, progesterone, FSH, and LH serve as reliable markers for these conditions [32]. In our investigation, hormonal assays and vaginal smears were employed to confirm POF. Comparison between the CPA-treated and the control groups revealed significantly elevated levels of FSH and LH, accompanied by markedly reduced levels of E2 and progesterone, consistent with POF indications. Previous research has identified a distinct endocrine profile in POF, potentially associated with natural apoptotic pathways in ovarian follicles [17]. Alterations in ovarian granulosa cell hormone secretion may result from CPA-induced damage to ovarian tissues, affecting folliculogenesis and leading to ovarian failure [33].

POI involves a depletion of ovarian reserves, reduction in the follicle pool, and subsequent follicular dysfunction, as evidenced by elevated FSH levels. Cyclophosphamide®-induced apoptosis of GCs, the primary E2 producers, can decrease E2 levels. This decline disrupts the negative feedback mechanism of the hypothalamic-pituitary axis, resulting in increased FSH secretion [34]. Conversely, rats treated with GIII exhibited a significant reduction in serum FSH and LH levels than the GII group. Additionally, estrogenic hormone levels in the GIII-treated group were comparable to those in the GI group. Although unable to persist long-term in target tissues, stem cells exert paracrine and autocrine effects, activating local stem cells and promoting healing [29].

Ovarian stromal stem cells (OSSCs) may offer superior protection for follicle maturation compared to BM-MSCs in cyclophosphamide-induced ovarian damage. MSCs influence damaged tissues directly and through paracrine and autocrine activities, releasing growth factors, proteins, immune modulators, and chemokines to aid in tissue recovery [21,29]. Additionally, embryonic stem cell-derived extracellular vesicles (ESC-sEVs) have effectively restored ovarian function in POI mouse models [35]. Quantitative histomorphometric analysis in our study demonstrated a significant rise in the average number of primordial follicles following BM-MSC applied compared to CPA chemotherapy. This corresponds with previous findings where adipose-derived stem cell (ADSC) treatment increased corpora lutea and the total number of follicles [19,36]. Higher doses of cyclophosphamide administration led to a notable decline in the number of primordial follicles; however, this reduction was partially attenuated by in vivo transplantation of BM-MSCs. Furthermore, Cyclophosphamide® applied caused a significant reduction in the count of secondary follicles, likely due to its cytotoxic effects on granulosa cells, which are pivotal in folliculogenesis [33,37].

Histological examinations indicated considerable ovarian damage post-chemotherapy, evidenced by follicular depletion and vascular modifications, likely driven by oxidative stress, inflammatory responses, and apoptotic processes [38][38]. Conversely, treatment with BM-MSCs facilitated follicular regeneration and mitigated ovarian damage, consistent with observations from prior studies [4].

5. Conclusions

This study demonstrated that BM-MSCs significantly enhance ovarian function, histopathological structure, and follicle development in CPA-induced POF rats through paracrine effects. Hormonal analysis showed CPA-induced hormonal imbalances and histological damage, which were notably restored by BM-MSC therapy. Specifically, BM-MSCs facilitated ovarian folliculogenesis and mitigated the deleterious effects of CPA. Histopathological assessment revealed substantial improvements in follicle counts and tissue integrity post-treatment. PKH-26 labelling confirmed successful BM-MSC engraftment in ovarian tissue, underscoring their therapeutic potential in chemotherapy-induced POF

Acknowledgment

The authors would like to thank Fayoum University for supporting the publication of this work.

Author Contributions

All authors contributed to this work. N. Sobhy prepared the samples and completed the experimental measurements. Both A. Atwa and S. Bakry shared writing and followed the performance of the experiments. A.M. Abdel Latif helped the first author complete the sample preparation. A.M. Abdel Latif with N. Sobhy completed the paper writing, analyzing the data, and validation. A. Atwa followed the revision and submission of the manuscript for publication.

Declaration of Competing Interest

The authors declare that they have no known competing financial interests or personal relationships that could have appeared to influence the work reported in this paper.

References

[1] M. Hansen, R.J. Hart, E. Milne, C. Bower, M.L. Walls, J.L. Yovich, P. Burton, Y. Liu, H. Barblett, A. Kemp-Casey, Ovulation induction and subfertile untreated conception groups offer improved options for interpreting risks associated with ART, J. Assist. Reprod. Genet., 41 (2024) 915–928.
[2] G. Sheikhansari, L. Aghebati-Maleki, M. Nouri, F. Jadidi-Niaragh, M. Yousefi, Current approaches for the treatment of premature ovarian failure with stem cell therapy, Biomed. Pharmacother., 102 (2018) 254–262.
[3] M.M. Barreca, P. Cancemi, F. Geraci, Mesenchymal and induced pluripotent stem cells-derived extracellular vesicles: the new frontier for regenerative medicine?, Cells, 9 (2020) 1163.
[4] S. Kilic, F. Pinarli, C. Ozogul, N. Tasdemir, G. Naz Sarac, T. Delibasi, Protection from cyclophosphamide-induced ovarian damage with bone marrow-derived mesenchymal stem cells during puberty, Gynecol. Endocrinol., 30 (2014) 135–140.
[5] S.A. Zahkook, A. Atwa, M. Shahat, A.M. Mansour, S. Bakry, Mesenchymal stem cells restore fertility in induced azoospermic rats following chemotherapy administration, J Reprod Infertil, 5 (2014) 50–57.
[6] M.H. Jazayeri, K. Barzaman, R. Nedaeinia, T. Aghaie, M. Motallebnezhad, Human placental extract attenuates neurological symptoms in the experimental autoimmune encephalomyelitis model of multiple sclerosis-a putative approach in MS disease?, Autoimmun. Highlights, 11 (2020) 1–9.
[7] A. Buigues, M. Marchante, S. Herraiz, A. Pellicer, Diminished ovarian reserve chemotherapy-induced mouse model: a tool for the preclinical assessment of new therapies for ovarian damage, Reprod. Sci., 27 (2020) 1609–1619.
[8] F. Han, J. Wang, L. Ding, Y. Hu, W. Li, Z. Yuan, Q. Guo, C. Zhu, L. Yu, H. Wang, Tissue engineering and regenerative medicine: achievements, future, and sustainability in Asia, Front. Bioeng. Biotechnol., 8 (2020) 83.
[9] J. Liang, M. E, G. Wu, L. Zhao, X. Li, X. Xiu, N. Li, B. Chen, Z. Hui, J. Lv, Nimotuzumab combined with radiotherapy for esophageal cancer: preliminary study of a Phase II clinical trial, Onco. Targets. Ther., (2013) 1589–1596.
[10] J. Johnson, J. Canning, T. Kaneko, J.K. Pru, J.L. Tilly, Germline stem cells and follicular renewal in the postnatal mammalian ovary, Nature, 428 (2004) 145–150.
[11] E.E. Telfer, R.G. Gosden, A.G. Byskov, N. Spears, D. Albertini, C.Y. Andersen, R. Anderson, R. Braw-Tal, H. Clarke, A. Gougeon, On regenerating the ovary and generating controversy, Cell, 122 (2005) 821–822.
[12] H. Aboutalebi, F. Alipour, A. Ebrahimzadeh-Bideskan, The protective effect of co-administration of platelet-rich plasma (PRP) and pentoxifylline (PTX) on cyclophosphamide-induced premature ovarian failure in mature and immature rats, Toxicol. Mech. Methods, 32 (2022) 588–596.
[13] E.A.H. Knauff, L. Franke, M.A. Van Es, L.H. Van den Berg, Y.T. Van der Schouw, J.S.E. Laven, C.B. Lambalk, A. Hoek, A.J. Goverde, S. Christin-Maitre, Genome-wide association study in premature ovarian failure patients suggests ADAMTS19 as a possible candidate gene, Hum. Reprod., 24 (2009) 2372–2378.
[14] M.E. El-Sayed, A. Atwa, A.R. Sofy, Y.A. Helmy, K. Amer, M.G. Seadawy, S. Bakry, Mesenchymal stem cell transplantation in burn wound healing: uncovering the mechanisms of local regeneration and tissue repair, Histochem. Cell Biol., 161 (2024) 165–181.
[15] S. Bhansali, V. Kumar, U.N. Saikia, B. Medhi, V. Jha, A. Bhansali, P. Dutta, Effect of mesenchymal stem cells transplantation on glycaemic profile & their localization in streptozotocin induced diabetic Wistar rats, Indian J. Med. Res., 142 (2015) 63–71.
[16] F. Torino, A. Barnabei, L. De Vecchis, M. Appetecchia, L. Strigari, S.M. Corsello, Recognizing menopause in women with amenorrhea induced by cytotoxic chemotherapy for endocrine-responsive early breast cancer, Endocr. Relat. Cancer, 19 (2012) R21–R33.
[17] M. Lappi, A. Borini, Fertility preservation in women after the cancer, Curr. Pharm. Des., 18 (2012) 293–302.
[18] A. Bukovsky, Ovarian stem cell niche and follicular renewal in mammals, Anat. Rec. Adv. Integr. Anat. Evol. Biol., 294 (2011) 1284–1306.
[19] Y. Takehara, A. Yabuuchi, K. Ezoe, T. Kuroda, R. Yamadera, C. Sano, N. Murata, T. Aida, K. Nakama, F. Aono, The restorative effects of adipose-derived mesenchymal stem cells on damaged ovarian function, Lab. Investig., 93 (2013) 181–193.
[20] G.-Y. Xiao, I.-H. Liu, C.-C. Cheng, C.-C. Chang, Y.-H. Lee, W.T.-K. Cheng, S.-C. Wu, Amniotic fluid stem cells prevent follicle atresia and rescue fertility of mice with premature ovarian failure induced by chemotherapy, PLoS One, 9 (2014) e106538.
[21] A. Uccelli, L. Moretta, V. Pistoia, Mesenchymal stem cells in health and disease, Nat. Rev. Immunol., 8 (2008) 726–736.
[22] O. Oktem, K. Oktay, A novel ovarian xenografting model to characterize the impact of chemotherapy agents on human primordial follicle reserve, Cancer Res., 67 (2007) 10159–10162.
[23] S. Morgan, R.A. Anderson, C. Gourley, W.H. Wallace, N. Spears, How do chemotherapeutic agents damage the ovary?, Hum. Reprod. Update, 18 (2012) 525–535.
[24] S.H. Abd-Allah, S.M. Shalaby, H.F. Pasha, S. Amal, N. Raafat, S.M. Shabrawy, H.A. Awad, M.G. Amer, M.A. Gharib, E.A. El Gendy, Mechanistic action of mesenchymal stem cell injection in the treatment of chemically induced ovarian failure in rabbits, Cytotherapy, 15 (2013) 64–75.

[25] D. Meirow, H. Biederman, R.A. Anderson, W.H.B. Wallace, Toxicity of chemotherapy and radiation on female reproduction, Clin. Obstet. Gynecol., 53 (2010) 727–739.
[26] S.M. Devine, C. Cobbs, M. Jennings, A. Bartholomew, R. Hoffman, Mesenchymal stem cells distribute to a wide range of tissues following systemic infusion into nonhuman primates, Blood, J. Am. Soc. Hematol., 101 (2003) 2999–3001.
[27] G. Forte, M. Minieri, P. Cossa, D. Antenucci, M. Sala, V. Gnocchi, R. Fiaccavento, F. Carotenuto, P. De Vito, P.M. Baldini, Hepatocyte growth factor effects on mesenchymal stem cells: proliferation, migration, and differentiation, Stem Cells, 24 (2006) 23–33.
[28] D.-J. Li, C.-A. Shen, T.-J. Sun, L. Zhang, H.-P. Deng, J.-K. Chai, Mesenchymal stem cells promote incision wound repair in a mouse model, Trop. J. Pharm. Res., 16 (2017) 1317–1323.
[29] H.E. Besikcioglu, G.S. Sarıbas, C. Ozogul, M. Tiryaki, S. Kilic, F.A. Pınarlı, O. Gulbahar, Determination of the effects of bone marrow derived mesenchymal stem cells and ovarian stromal stem cells on follicular maturation in cyclophosphamide induced ovarian failure in rats, Taiwan. J. Obstet. Gynecol., 58 (2019) 53–59.
[30] A. Atwa, M.R. Sofy, S.M. Fakhrelden, O. Darwish, A.B.M. Mehany, A.R. Sofy, S. Bakry, Biodegradable materials from natural origin for tissue engineering and stem cells technologies, in: Handb. Biodegrad. Mater., Springer, 2022: pp. 1–40.
[31] A. Atwa, A.K.M. Abdel Latif, M.A. Moustafa, M. Ashry, H. Askar, A.Z.I. Shehata, A.B.M. Mehany, S.I. Hallool, S. Bakry, Integrating Nanosensors into Stem Cells Technologies and Regenerative Medicine, in: Handb. Nanosensors Mater. Technol. Appl., Springer, 2024: pp. 1113–1147.
[32] V. Wesevich, A.N. Kellen, L. Pal, Recent advances in understanding primary ovarian insufficiency, F1000Research, 9 (2020) 12688.
[33] N.M. Abogresha, S.S. Mohammed, M.M. Hosny, H.Y. Abdallah, A.M. Gadallah, S.M. Greish, Diosmin mitigates cyclophosphamide induced premature ovarian insufficiency in rat model, Int. J. Mol. Sci., 22 (2021) 3044.
[34] K. Yacobi, A. Wojtowicz, A. Tsafriri, A. Gross, Gonadotropins enhance caspase-3 and-7 activity and apoptosis in the theca-interstitial cells of rat preovulatory follicles in culture, Endocrinology, 145 (2004) 1943–1951.
[35] H. Liu, X. Wei, Y. Sha, W. Liu, H. Gao, J. Lin, Y. Li, Y. Tang, Y. Wang, Y. Wang, Whole-exome sequencing in patients with premature ovarian insufficiency: early detection and early intervention, J. Ovarian Res., 13 (2020) 1–8.
[36] G. Ai, M. Meng, J. Guo, C. Li, J. Zhu, L. Liu, B. Liu, W. Yang, X. Shao, Z. Cheng, Adipose-derived stem cells promote the repair of chemotherapy-induced premature ovarian failure by inhibiting granulosa cells apoptosis and senescence, Stem Cell Res. Ther., 14 (2023) 75.
[37] D. Song, Y. Zhong, C. Qian, Q. Zou, J. Ou, Y. Shi, L. Gao, G. Wang, Z. Liu, H. Li, Human umbilical cord mesenchymal stem cells therapy in cyclophosphamide-induced premature ovarian failure rat model, Biomed Res. Int., 2016 (2016) 2517514.
[38] R.S. Barberino, R.L.S. Silva, R.C. Palheta Junior, J.E.J. Smitz, M.H.T. Matos, Protective effects of antioxidants on cyclophosphamide-induced ovarian toxicity, Biopreserv. Biobank., 21 (2023) 121–141.